Path deviation control for multi-UAV cooperative task execution based on laser vision guidance and trajectory prediction

Jingjing Liao
Chengdu College of University of Electronic Science and Technology of China, Chengdu, 610000, China
E-mail: *liao606952@163.com*

Received 30 June 2025; accepted 2 May 2026; published online 27 September 2026
DOI https://doi.org/10.21595/jme.2026.25171

Check for updates

Abstract. This paper proposes a path deviation control method that integrates laser vision guidance and trajectory prediction to address deviations caused by limited environmental perception in multi-drone cooperative tasks. First, a local 3D point cloud map is constructed using Light Detection and Ranging (LiDAR). Global environment modeling is achieved through Oriented FAST and Rotated BRIEF Simultaneous Localization and Mapping 3 (ORB-SLAM3) and a multi-agent cooperative mapping mechanism. Second, multidimensional constraints, including turning radius, velocity, and safety distance of the unmanned aerial vehicles (UAVs), are incorporated into an improved A* algorithm to enhance the accuracy and feasibility of trajectory prediction. Finally, real-time path correction is realized using a fuzzy proportional-integral-derivative (PID) controller, forming a closed "perception-planning-control" loop. Experimental results show that the proposed method achieves a path deviation of only 1.0 m, reduces task time to 10 min, and maintains a collision rate as low as 2 %. It remains stable under complex conditions such as Global Positioning System (GPS) denial and strong winds. The method significantly improves path accuracy, stability, and obstacle avoidance capability in multi-drone cooperative tasks and can be widely applied in fields such as logistics distribution, disaster monitoring, and cooperative inspection.

Keywords: laser vision guidance, trajectory prediction, multi-UAV, cooperative tasks, path deviation control, cooperative map construction.

1. Introduction

Currently, unmanned aerial vehicle (UAV) technology is widely applied in practice owing to its high efficiency, flexibility, and ability to enable cooperative operations among unmanned clusters, particularly in fields such as agriculture, military, and logistics [1]. In real-world scenarios, multiple drones cooperating to perform tasks can fully leverage the advantages of UAV clusters, ensuring high efficiency and quality of task execution [2]. With the continuous advancement of information technology and digitalization, the application scope of UAVs keeps expanding. This is especially evident when multiple drones are employed to cooperate in task execution. Due to complex application environments, interference from various external factors, and equipment failures [3], certain deviations may occur in the flight paths of multiple drones. Once a path deviation arises, it reduces the efficiency and accuracy of task execution and may also lead to inter-drone collisions, resulting in safety incidents and economic losses [4]. Therefore, a path deviation control method for multi-drone cooperative task execution not only helps improve the quality and efficiency of UAV task performance but also promotes the further development of UAV control technology, which is of considerable significance.

Trad et al. introduced deep reinforcement learning and proposed a multi-UAV path deviation control method [5]. The method described drone positions and states using a state space and then determined motion strategies via an action space based on environmental parameters, thereby achieving an optimal motion path. After determining the optimal action of the drone using the Deep Q-Network (DQN) deep reinforcement learning algorithm, the model was iteratively updated to accomplish deviation calculation and control. However, in practical applications, it has been found that this method struggled to cope with the impact of complex external environments on deviation control, leading to degraded quality of path deviation control. Shiri et al. introduced an attention mechanism and proposed a multi-UAV path deviation control method [6]. Multiple sensors collected drone operation data. The collected data were normalized and cleaned. Key operational features were then extracted to determine the drone's actual state and path deviation. Once the path deviation was determined, a drone path deviation control model based on the attention mechanism was constructed. The extracted key features were input into the model, which then determined the drone position and attitude adjustment strategy according to the actual situation and executed the adjustment strategy to optimize the control of the drone, thereby accurately reducing path deviation. However, practical tests revealed that this method did not account for the cooperative relationships among multiple drones, making collisions between them likely. Consequently, there was a significant gap between the practical performance of this method and the expected goal. Sakai et al. comprehensively considered data-driven dual-rate cascade control of pitch angle and designed a novel UAV path deviation control method [7]. Historical flight data were used to train a data-driven model, and a dual-rate cascade control system was constructed. In this system, the outer loop controlled the pitch angle while the inner loop controlled the pitch rate, achieving fast response and precise control. Nevertheless, practical testing showed that the pitch angle calculated by this method deviated significantly from the actual value, and its control quality was consequently not high. Xin et al. proposed a drone control method based on real-time deep-learning object detection [8]. Cameras installed on each drone performed real-time object detection using the You Only Look Once (YOLO) deep-learning model. The YOLO object detector continuously estimated the relative position of the UAV ahead, and based on this position, each drone was controlled by a proportional-derivative (PD) feedback controller to achieve formation control. Sun et al. proposed an intelligent distributed UAV control method based on optical flow sensors [9]. This method addressed the issues of high cost and relatively fixed operating environment associated with GPS, optical motion capture, or other positioning methods used for distributed drones. Using optical flow sensors, drone systems could achieve high-precision, low-cost autonomous positioning, real-time obstacle avoidance, and hover correction, thereby realizing an intelligent distributed UAV control method.

Although some progress has been made in controlling path deviation for multiple drones, limitations remain. These include incomplete environmental perception and the fact that trajectory prediction insufficiently considers UAV physical constraints and dynamic coordination. Furthermore, control strategies lack adequate adaptability in complex environments. This paper presents a path deviation control method for multi-UAV cooperative task execution based on laser vision guidance and trajectory prediction. The limitations of existing research are summarized in Table 1.

Table 1. Analysis of limitations in existing studies

Method	Main content	Research limitations and gaps
Trad et al. (2024)	Path control based on deep reinforcement learning (DQN) optimizes drone flight strategy through state action reward mechanism	Relying heavily on simulation training and lacking generalization ability; Without integrated real-time environmental perception, it is difficult to cope with dynamic obstacles and weather changes
Shiri et al. (2022)	Multi drone path planning using attention mechanism, achieving collaborative control through feature extraction and attention weight allocation	Not considering the dynamic coupling and physical constraints between drones; Conflicts and collision risks are prone to occur in multi machine intensive scenarios
Sakai et al. (2022)	Data driven dual rate cascade pitch angle control achieves path tracking through the coordination of the outer and inner loops	Without integrating environmental perception information, the control effect is limited in complex or dynamic environments with obstacles

Xin et al. (2023)	Real time object detection and PD controller based on YOLO deep learning model for unmanned aerial vehicle formation control	Dependent on visual sensors, greatly affected by lighting and occlusion; Strong communication dependency, prone to instability in complex environments
Sun et al. (2023)	Intelligent distributed control method based on optical flow sensors to achieve low-cost autonomous positioning and hover correction	Limited applicability scenarios, relying on ground texture features; Weak wind resistance and insufficient adaptability to outdoor dynamic environments
This work	Laser vision fusion mapping (LeGo LOAM+ORB-SLAM3)+multi constraint improved * trajectory prediction+fuzzy PID closed-loop control, achieving full process collaborative control from environmental perception, trajectory planning to real-time correction.	To address most of the limitations mentioned above, the innovation of the proposed method is as follows: 1. By fusing data from multiple sensors, it can effectively enhance the real-time performance of environmental perception and robust anti-interference ability; 2. In the trajectory prediction stage, embedding the dynamic characteristics and collaborative constraints of the drone can significantly improve the feasibility of the generated trajectory; 3. Design a closed-loop control architecture that enables the system to have stronger stability and adaptability in the face of various disturbances; 4. Through on-site verification of multi machine collaborative tasks, the system has demonstrated better performance than the comparative methods in key indicators such as path accuracy, task execution time, and collision occurrence rate.

Although some progress has been made in the control of path deviation for multiple drones, limitations remain, including incomplete environmental perception, insufficient consideration of drone physical constraints and dynamic coordination in trajectory prediction, and inadequate adaptability of control strategies in complex environments. Unlike the above methods, the method proposed in this paper has essential differences in the following aspects: the method based on deep reinforcement learning in [5] relies heavily on simulation training and does not integrate real-time environment perception; the method based on attention mechanism in [6] does not consider the dynamic coupling and physical constraints between UAVs; and the method based on data-driven cascade control in [7] does not integrate environment perception information. The novelty of this method lies in the first-time organic combination of laser vision fusion mapping technology, an A* trajectory prediction method improved with multi-constraint considerations, and a fuzzy PID closed-loop control strategy, forming a full-process collaborative control framework: at the perception level, high-precision global collaborative maps are constructed through the tight coupling fusion of LeGO-LOAM and ORB-SLAM3; at the planning level, multidimensional constraints such as turning radius, speed boundary, and safe distance between drones are embedded into the cost function of the improved A* algorithm; at the control level, real-time correction is achieved by using the deviation between the predicted trajectory and the actual position as the input to the fuzzy PID controller. This complete closed-loop architecture of “perception-planning-control” differs from the limitations of existing methods that separate perception and control, neglect physical constraints in planning, or lack environmental feedback in control, thus achieving significant improvements in key performance metrics such as path accuracy, system stability, and obstacle avoidance ability.

Laser vision guidance represents a state-of-the-art navigation technology that employs laser emission and reception modules along with visual sensors to achieve high-precision positioning and accurate navigation of UAVs [10]. Compared with traditional GPS navigation, laser vision guidance is unaffected by weather conditions and light intensity, providing stable navigation information even in complex environments. Moreover, when integrated with trajectory prediction technology, it can further pre-plan flight paths for drones, effectively avoiding potential collision risks and thus improving task execution efficiency. Therefore, applying laser vision guidance and trajectory prediction technology to the path deviation control stage in multi-UAV cooperative task execution can enhance the overall performance of the UAV system. The novelty of the proposed method lies in establishing a full-process cooperative control framework that combines laser-vision-based fusion mapping, an improved trajectory prediction method incorporating multiple constraints, and a fuzzy-PID closed-loop control strategy. It successfully overcomes limitations of existing methods, such as incomplete environmental perception and insufficient consideration of UAV physical constraints and dynamic cooperative requirements in trajectory prediction, while addressing the poor adaptability of control strategies in complex environments. The method first achieves high-precision perception of complex environments through multi-drone cooperative mapping. Second, by incorporating multidimensional factors - including minimum turning radius, minimum path length, flight speed conditions, and spatial constraints - the improved A* algorithm achieves trajectory prediction that better complies with UAV dynamic and coordination requirements. Finally, a closed-loop deviation control mechanism based on a fuzzy control algorithm and a PID speed control algorithm enables rapid response and accurate correction of path deviations, thereby enhancing the overall cooperative performance of multi-UAV systems in dynamic and complex environments while improving path control accuracy, system stability, and obstacle-avoidance capability. The method demonstrates significant practical value in scenarios such as industrial inspection, logistics distribution, and disaster management. For industrial inspection tasks including power line inspection and infrastructure monitoring, it enables high-precision, high-coverage cooperative operations in complex, unstructured environments, effectively reducing manual involvement and operational risks. In emergency logistics and urban distribution scenarios, by relying on accurate trajectory prediction and real-time deviation control, the method ensures safe and efficient passage of multiple drones in dense and dynamically changing obstacle environments, greatly improving the success rate and timeliness of material delivery. In disaster monitoring and search-and-rescue applications, the system maintains stable operation under harsh conditions such as GPS signal denial and sensor interference, providing strong support for UAV clusters to perform stable cooperative surveys and real-time situational awareness in complex post-disaster terrain. Overall, through full-chain optimization of environmental perception, trajectory planning, and control execution, the method offers a feasible technical pathway for large-scale, highly reliable cooperative operation of multi-UAV systems in real-world industrial and emergency scenarios.

2. Theoretical and industrial/management implications

2.1. Theoretical implications

This study proposes an integrated multi-drone cooperative control framework at the theoretical and methodological levels, with the following key contributions.

First, in multi-sensor fusion and simultaneous localization and mapping (SLAM), this work innovatively combines the Length- and Ground-Optimized Lidar Odometry and Mapping on Variable Terrain (LeGO-LOAM) algorithm with the Oriented FAST and Rotated BRIEF Simultaneous Localization and Mapping 3 (ORB-SLAM3) algorithm to construct a cooperative mapping method suitable for multiple drones. This approach not only enhances the real-time performance and accuracy of local maps but also addresses map alignment and drift-correction issues in multi-view, multi-source data through a unified world coordinate system and map-fusion mechanism, thereby laying a reliable foundation for future path planning and control in dynamic environments. Second, regarding trajectory prediction, the study improves the classical A* algorithm by incorporating multidimensional constraint fusion. The dynamic characteristics of UAVs and environmental constraints are embedded into the cost function, and a dynamic weight-adjustment mechanism is introduced, enabling the algorithm to maintain high efficiency and adaptability in complex dynamic settings. This provides an extensible heuristic-search framework for multi-agent cooperative path planning. Finally, at the control-strategy level, an integrated closed-loop control process combining fuzzy logic and PID control is constructed, achieving rapid response and accurate correction of path deviations and offering theoretical and methodological support for robust control of multi-UAV systems in uncertain environments.

2.2. Industrial and management implications

Industry refers to economic sectors that utilize science, technology, equipment, and manpower to engage in the production, processing, and construction of material products, including manufacturing, energy, mining, and construction. Management denotes the process of coordinating human, material, financial, and information resources through functions such as planning, organizing, leading, and controlling to achieve organizational goals. The method proposed in this study holds significant practical value for industrial applications and operational management.

At the industrial application level, the method can be widely employed in scenarios such as emergency logistics distribution, urban inspection, agricultural crop protection, and disaster monitoring. For example, in emergency material distribution, it enables precise, efficient, and safe cooperative flight in complex urban environments, thereby substantially improving the efficiency and reliability of material delivery. When applied to power-line inspection or infrastructure monitoring, multiple drones can cooperate to complete large-scale, high-precision data-collection tasks, effectively reducing labor costs and operational risks. Moreover, the method maintains stable operation under harsh conditions such as GPS signal loss and sensor interference, further enhancing the applicability and anti-interference robustness of UAV systems in real-world industrial environments.

From a management perspective, the proposed method provides solid and robust technical support for multi-drone clusters in task scheduling, resource allocation, and cooperative efficiency management. Through real-time trajectory prediction and deviation control, managers can achieve dynamic monitoring and intelligent scheduling of drone clusters, optimize task execution sequences and path planning, reduce collision risks and energy consumption, and improve overall task execution efficiency. Furthermore, the method supports flexible scaling of the number of drones, with low memory usage and high system stability, which facilitates centralized control and distributed cooperation of large-scale drone clusters. This offers a feasible technical pathway and management paradigm for UAV operation and management in future domains such as smart logistics and smart cities.

3. Path deviation control method for multi-UAV cooperative task execution

The process architecture of path deviation control for multi UAV collaborative task execution based on laser vision guidance and trajectory prediction is shown in Fig. 1.

The process of path deviation control for multi-UAV collaborative task execution based on laser vision guidance and trajectory prediction is as follows:

First, in the perception layer, each drone is equipped with LiDAR and visual sensors, and the LeGO-LOAM algorithm is used for point cloud segmentation, feature extraction, radar odometry calculation, and loop detection to generate local 3D point cloud maps. Then, a unified world coordinate system is established through the ORB-SLAM3 framework, and the local maps are fused into a global collaborative task map based on a keyframe consensus mechanism and the ICP registration algorithm. Second, at the planning level, the lower limits of the turning radius, path length, flight speed conditions, inter-UAV safety distance, and obstacle avoidance space constraints are embedded into the cost function of the improved A* algorithm. The optimal trajectory set that meets the dynamic characteristics of the UAVs and the requirements of multi-UAV coordination is generated through a dynamic weight adjustment mechanism. Finally, in the control layer, the predicted trajectory is compared with the actual flight position to calculate the angle deviation and center distance deviation. These two deviations are used as inputs for the fuzzy controller, and after fuzzy inference, PID control parameters are output to drive the drone to perform corrective actions, forming a closed-loop feedback link of "perception-planning-control".

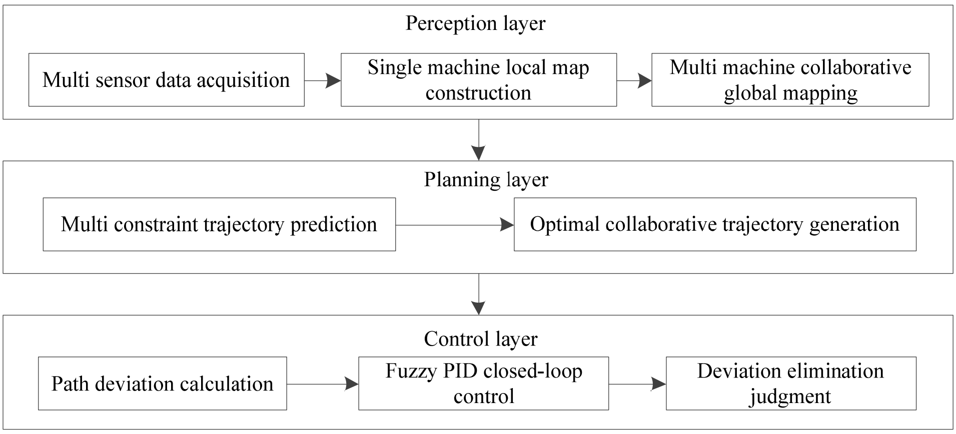

Fig. 1. Process architecture of path deviation control for multi-UAV collaborative task execution based on laser vision guidance and trajectory prediction

3.1. Cooperative map construction for multi-UAV systems based on laser vision guidance

The construction of a three-dimensional map for multi-UAV cooperative tasks using laser vision guidance imposes specific requirements on the mapping algorithm, as it must coordinate multi-UAV cooperative actions while demonstrating high tolerance to drift errors and maintaining real-time performance. After comprehensive evaluation, the LeGO-LOAM algorithm is selected. It is used for individual UAV local map construction based on laser vision guidance. The architecture for constructing a local map of a single UAV using this guidance approach is shown in Fig. 2.

Fig. 2 illustrates the process of constructing a local map for a single UAV based on laser vision guidance. The process adopts the LeGO-LOAM algorithm framework, which is divided into front-end and back-end parts. Starting from the point cloud data acquired by LiDAR scanning, the front-end sequentially performs point cloud segmentation, feature extraction, LiDAR odometry computation, and loop-closure detection to estimate the UAV's pose changes in real time and extract environmental features. The back-end then applies pose-graph optimization to the pose estimates from the front-end, performing global consistency correction to effectively reduce accumulated errors. Finally, the optimized pose information is used for map construction and updating, generating an accurate local 3D point cloud map. The entire process forms a complete closed loop from data acquisition and feature processing to optimized mapping.

The Lightweight and Ground-Optimized Lidar Odometry and Mapping on Variable Terrain (LeGO-LOAM) algorithm is a specialized light detection and ranging (LiDAR) odometry and mapping method designed primarily for real-time six-degree-of-freedom (6DOF) pose estimation. Developed as an optimization of the LOAM framework, it enables real-time pose estimation for UAVs even on low-power embedded systems.

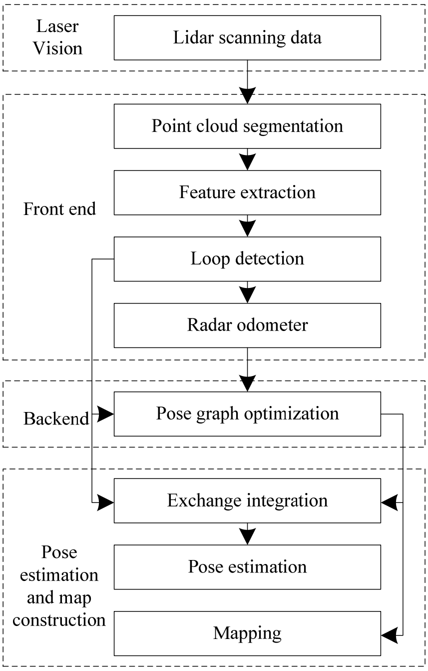

Fig. 2. Process for constructing a local map of a single UAV based on laser vision guidance

During the local map construction for a single UAV using the LeGO-LOAM algorithm, three-dimensional point-cloud data of the surrounding environment are acquired by a LiDAR sensor mounted on the drone. The front-end processing comprises four key steps: point-cloud segmentation, feature extraction, LiDAR odometry, and loop-closure detection [11]; the back-end carries out pose-graph optimization. Through the joint operation of the front-end and back-end, the system significantly reduces the UAV's drift error and enhances the real-time performance of local 3D point-cloud map generation. In the feature-extraction stage, smoothness is computed using Eq. (1):

$$c = \frac{1}{|S| \cdot |r_{ki}|} \left\| \sum_{j \in S, j \neq i} \left(r_{kj} - r_{ki} \right) \right\|. \tag{1}$$

Depth information is denoted by r_{ki}, while the set of points consisting of a specific point in the laser point cloud and five adjacent points on each side within the same row is represented by S [12]. Subsequently, in the LiDAR odometry stage, iterative processing is carried out using Eq. (2):

$$W_k \leftarrow W_k - \left(J^T + diag(J^T J) \right)^{-1} J^T h, \tag{2}$$

where, J denotes the Jacobian matrix, W_k represents the pose estimate, and h has a dual interpretation: it refers both to the distance between edge features and to the distance for the planar feature set.

In the back-end design, the UAV pose-graph objective function enables the acquisition of accurate UAV pose transformation data:

$$\min W = \frac{1}{2} \sum_{(i,j) \in \varepsilon} e_{ij}^T \sum_{ij}^{-1} e_{ij}. \tag{3}$$

The pose estimates of all pose nodes are denoted by W; the set of all edges is denoted by ε; the pose estimation error is denoted by e_{ij}; and the covariance matrix is denoted by $\sum_{ij}$.

Following the acquisition of the UAV's pose transformation results, the system performs final loop-closure detection and map construction to generate the completed local 3D point-cloud map. The proposed map-construction method for laser-vision-guided multi-UAV cooperative systems integrates local 3D point-cloud maps by establishing a unified world coordinate system for each UAV.

(I) World Coordinate System Establishment.

ORB-SLAM3 (Oriented FAST and Rotated BRIEF Simultaneous Localization and Mapping) is an open-source real-time visual SLAM system, developed by extending and enhancing ORB-feature-based 3D localization and mapping algorithms such as ORB-SLAM2 and ORB-SLAM-VI, with compatibility for various camera configurations. The ORB-SLAM3 framework incorporates a DBoW2 (Database of Words) database to store keyframes captured by the multi-UAV laser-vision systems. The pose transformation between adjacent keyframes can be computed using Eq. (3). The construction of the world coordinate system for each UAV involves the following steps:

1) Position multiple UAVs performing cooperative tasks with aligned LiDAR orientations to establish inter-system consensus [13] and ensure sufficient feature-point acquisition.

2) Initialize each UAV's LiDAR system and store the processed keyframes in the DBoW2 database through ORB-SLAM3.

3) The keyframes stored in the DBoW2 database serve as reference frames for each UAV to build its world coordinate system.

4) After establishing their respective world coordinate systems, the UAVs generate a cooperative task-execution map.

(II) Multi-UAV Cooperative Map Fusion.

After obtaining world coordinate systems from their respective local 3D point-cloud mapping systems, the UAVs employ the RGB-L-integrated ORB-SLAM3 algorithm to produce a cooperative task-execution map. The fusion process is illustrated in Fig. 3.

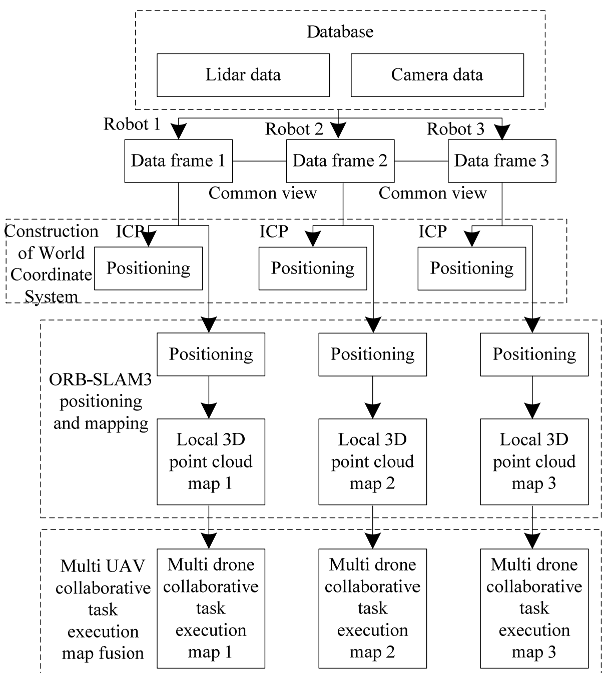

Fig. 3. Map fusion framework for multi-UAV cooperative task execution

ISSN PRINT 2335-2124, ISSN ONLINE 2424-4635

The multi-UAV cooperative task map-fusion process consists of three key steps:

(1) Retrieving local 3D point-cloud maps and camera images from the keyframe database using laser-vision guidance;

(2) Establishing coordinate transformations through the keyframe-tracking model and the Iterative Closest Point (ICP) algorithm when camera-image consensus is reached, followed by world-coordinate-system creation via Robot Operating System 2 (ROS2) data-transmission topics;

(3) Acquiring UAV pose states and performing loop-closure detection to generate the final local 3D point-cloud map.

Based on the world coordinate system defined in step (2), each local map is transformed using the pose-transformation relationship [14], projecting it into the world coordinate system and integrating it into a multi-UAV cooperative task-execution map.

In the multi-UAV cooperative task-execution map constructed through the above process, an improved A* algorithm is employed for multi-UAV trajectory prediction to generate the cooperative task-execution path, while path-deviation control is achieved by comparing the predicted path with the target path.

3.2. Trajectory prediction for multi-UAV cooperative tasks based on an improved A* algorithm

Fig. 4 illustrates the path-deviation control process for multi-UAV cooperative task execution based on trajectory prediction.

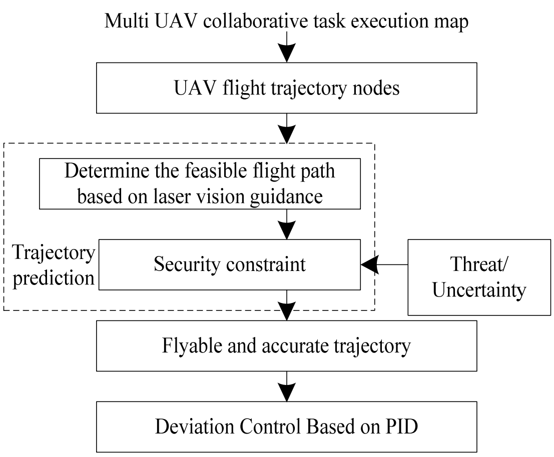

Fig. 4. Path deviation control process for multi-UAV cooperative task execution

Fig. 4 illustrates the complete path-deviation control process for multi-UAV cooperative task execution based on trajectory prediction. First, a feasible flight path is determined by constructing a multi-UAV cooperative task map and defining flight-trajectory nodes using laser-vision guidance. Then, a trajectory-prediction module that incorporates safety constraints as well as threat and uncertainty factors generates a feasible and accurate cooperative trajectory. Finally, the deviation between the predicted trajectory and the actual flight position is fed into a PID controller to achieve closed-loop path correction, forming a complete deviation-suppression chain that spans environmental perception, trajectory planning, and real-time control. The multi-UAV cooperative task-execution path-deviation control builds upon the single-UAV trajectory-prediction algorithm [15] and integrates multiple constraints and objective functions for cooperative trajectory prediction. These include collision-avoidance constraints and inter-agent information-sharing constraints [16], while the objective function aims either to minimize the total operational cost of the UAV swarm or to maximize simultaneous target arrival. This framework enables the acquisition of optimal trajectory-prediction data for multi-drone cooperative task execution. The prediction result is compared with the drone's actual position to accurately calculate the deviation. The deviation value is then input to the PID controller. By leveraging the regulating capability of the PID controller, path deviation can be effectively corrected, ensuring stable flight of the drone along the predefined route.

The A* algorithm employs a heuristic strategy that combines characteristics of Dijkstra's algorithm and the greedy algorithm. It leverages the advantage of Dijkstra's algorithm in precisely exploring globally optimal paths while also adopting the greedy algorithm's ability to rapidly approach the target during the search process, thereby enabling efficient and accurate prediction of the optimal trajectory [17-18]. As a classical heuristic algorithm for trajectory prediction, the A* algorithm incorporates heuristic information throughout its computation [19-20]. Its evaluation function is given by:

$$f(i) = g(i) + u(i), \tag{4}$$

where, i denotes an arbitrary node in the trajectory-prediction process. $f(i)$ represents the evaluation function for trajectory generation, indicating the total trajectory cost from the start to the target via node i. $g(i)$ corresponds to the actual trajectory cost (distance) for the UAV to travel from the start to node i in the flight environment, while $u(i)$ denotes the heuristic function that estimates the optimal trajectory cost from node i to the target point.

The A* algorithm can find an optimal solution under specific conditions [21]. To guarantee optimality, the heuristic function $u(i)$ used by the A* algorithm must be admissible, meaning it must never overestimate the actual cost $g(i)$ to reach the goal. If $u(i)$ is always less than or equal to $g(i)$, the algorithm is guaranteed to find the optimal solution. However, if $u(i)$ overestimates $g(i)$, optimality cannot be ensured.

To enhance the performance of trajectory prediction in multi-drone cooperative task execution and minimize path deviation, the A* algorithm is improved based on its actual cost function. Specifically, the optimization of the actual cost function incorporates multiple factors, including the minimum turning radius, the minimum path length, specific velocity requirements, and spatial constraints of the UAV [22-23]. The detailed procedure is provided in the Appendix.

During cooperative task execution, assuming that each drone maintains a constant-speed flight state, its flight distance and flight time exhibit a proportional relationship. Consequently, the distance between different drones can be derived by calculating the position of each drone at a specific time point t.

Based on the above analysis, the trajectory for cooperative task execution is predicted. The flight trajectories predicted by the improved A* algorithm during multi-drone cooperative task execution, together with the inter-drone deviation data, serve as input to the PID controller, enabling effective control of path deviation in multi-drone cooperative task execution [24].

Simultaneously, a dynamic weight-adjustment mechanism is introduced into the algorithm. This mechanism can adjust the influence weights of various constraints on the cost function in real time and flexibly, depending on different task scenarios and the specific performance of the drone. This process enhances the adaptability and flexibility of the algorithm. In handling spatial constraints, the algorithm calculates the position of each drone in real time, dynamically ensures a safe distance between drones, and maintains a minimum safe distance between drones and obstacles. It can effectively cope with complex and varying flight environments, significantly improving the safety and reliability of trajectory planning. Moreover, by comprehensively considering multidimensional constraints, the algorithm also optimizes the heuristic function to produce a more accurate estimate of the optimal-path cost from the current node to the target node, thereby accelerating convergence to the optimal solution.

Overall, the improved A* algorithm achieves substantial improvements in the accuracy, efficiency, safety, and reliability of trajectory planning across multiple key dimensions, providing essential algorithmic support for path-deviation control in multi-UAV cooperative task execution.

The research objective is to verify the effectiveness of the improved A* algorithm in predicting trajectories for multi-UAV cooperative tasks, and to conduct comparative experiments with three alternative trajectory-prediction methods: the Model Predictive Control (MPC)-based trajectory-length method combining optimization and learning, the deep-learning-based trajectory-prediction method, and the improved Rapidly-exploring Random Tree star (RRT*)-based trajectory-prediction method. In the experiment, the trajectory length between the predicted endpoint and the target position obtained by each method is recorded and compared; the results are presented in Table 1.

Table 2. Predicted trajectory lengths between endpoints and target positions using different methods (m)

Drone Number	Improve the trajectory length of the A* algorithm	MPC trajectory length based on optimization and learning	Trajectory length based on deep learning	Trajectory length based on improved RRT* algorithm
UAV1	125.6	132.4	140.2	136.8
UAV2	118.3	126.7	135.1	131.5
UAV3	130.2	138.9	145.6	139.7

According to the analysis in Table 2, on all tested drones the trajectory length predicted by the improved A* algorithm is shorter than those obtained by the optimization-and-learning-based MPC method, the deep-learning method, and the improved RRT* algorithm. Its average trajectory length is 124.7 m, which is 6.0 %, 11.1 %, and 8.3 % shorter than the lengths produced by the MPC, deep-learning, and improved RRT* methods, respectively, indicating higher prediction accuracy. This improvement mainly stems from the deep integration of multidimensional constraints in the improved A* algorithm, which incorporates both the dynamic characteristics of UAVs and spatial safety requirements into the cost function, thereby avoiding the path redundancy or feasibility risks caused by fragmented constraint handling in traditional methods. The dynamic weight-adaptation mechanism of the algorithm can adjust constraint weights in real time according to the task objectives; for example, it reduces safety-distance weights to shorten paths in emergency tasks, whereas the MPC and deep-learning methods employ fixed weights and the improved RRT* algorithm relies on manually set parameters, which lack such flexibility. Furthermore, the algorithm intelligently optimizes the heuristic function by implicitly incorporating multiple constraints into the path-cost estimation, which improves search efficiency and overcomes the problems of local optima in the conventional A* algorithm and the low search efficiency of the improved RRT* algorithm.

3.3. Path deviation control based on PID

The UAV adjusts its movement direction according to the trajectory generated by the A* algorithm through a path-control cycle that follows the sequence perception → decision → execution → correction. During cooperative operations, trajectory deviations may arise due to obstacles or environmental disturbances, requiring corrective directional adjustments. Based on the UAV control-system architecture, a path-deviation control methodology that integrates fuzzy logic with PID speed-control algorithms is developed [25-26], as illustrated in Fig. 5.

In Fig. 5, $\Delta\alpha$ denotes the angular deviation between the UAV and the predicted trajectory, and Δq represents the lateral-distance deviation between the UAV and the predicted trajectory. The fuzzy-control algorithm performs path-deviation correction over multiple control cycles [27-28]. For each adjustment cycle, the algorithm takes $(\Delta\alpha_t, \Delta q_t)$ as input parameters, where $\Delta\alpha_t$ is the angular-deviation input for the t-th cycle and Δq_t is the lateral-distance-deviation input for the t-th cycle [29-30]. In summary, the path-deviation control process for multi-UAV cooperative task execution based on laser-vision guidance and trajectory prediction is illustrated in Fig. 6.

Fig. 6 illustrates the complete path-deviation control process for multi-UAV cooperative task execution based on laser-vision guidance and trajectory prediction. First, a local 3D point-cloud map is constructed through multi-sensor data acquisition, and a global cooperative task map is generated. Then, an A* algorithm is employed to predict the cooperative trajectory of multiple UAVs, producing the optimal cooperative trajectory under multi-constraint fusion. Subsequently, control commands are generated via fuzzy logic, and UAV attitude control is implemented using a PID controller. After verifying whether the path deviation has been eliminated, the UAV is guided to the target point. Finally, the entire task-execution process – from environmental perception and cooperative map construction through trajectory prediction to closed-loop control – is completed.

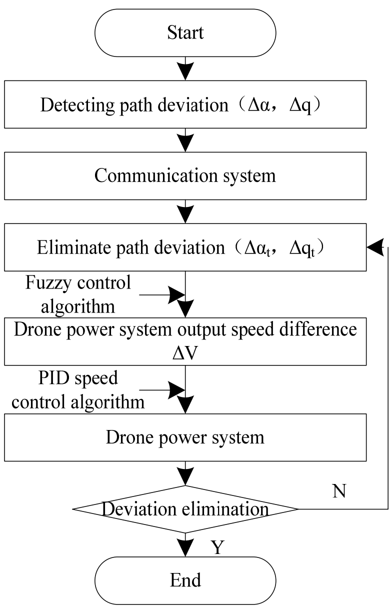

Fig. 5. Implementation process of the PID-based UAV path deviation control algorithm

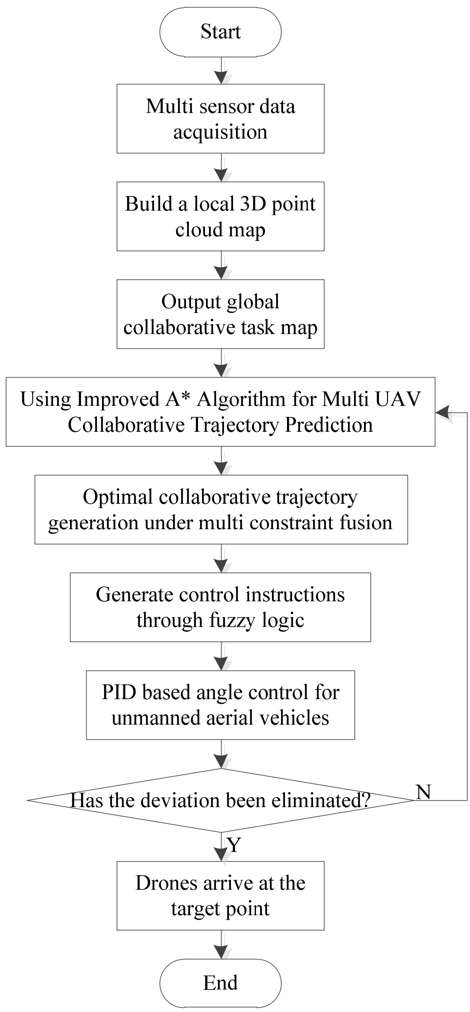

Fig. 6. Path deviation control process for multi-UAV cooperative task execution based on laser vision guidance and trajectory prediction

4. Experimental results

This paper investigates a laser-vision-guided path-deviation control method for multi-UAV cooperative task execution based on trajectory prediction. To evaluate the practical performance of the method, a multi-UAV cooperative emergency-supply-delivery task in an urban environment is selected as the test scenario (as shown in Fig. 7). The JDX-20 “Jingque” UAV model serves as the test platform, and its specifications are detailed in Table 3. The proposed method is experimentally validated by performing path-deviation control tests on the test platform during cooperative task execution.

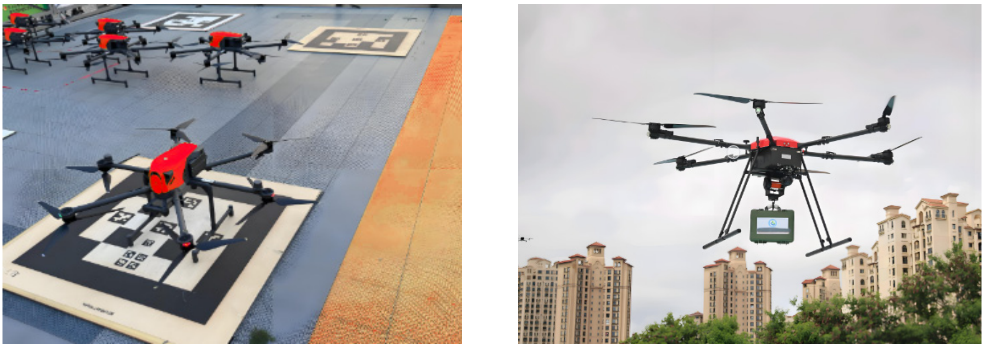

a) UAV base station b) UAV delivery

Fig. 7. Experimental environment for multi-UAV collaborative delivery tasks

Table 3. Parameters related to the research object

Parameter	Data
Drone model	JDX20 “Jingque”
Equipped with laser radar model	Riegl-240
Weight (kg)	10.9 (empty machine)
Viewing angle (°)	75 (bandwidth 1.53, maximum distance 1.25)
Accuracy (m/°)	Heading 0.035; Pitch and roll real-time 0.015
Ranging (m)	2150 (80 % measurement range)
Maximum flight speed (km/h)	98
Maximum flight mileage (km)	24
Maximum payload (kg)	10
Container capacity (L)	> 20
Endurance (min)	Not provided
Wind loading	Level 6 strong wind
Positioning accuracy (m)	Not provided
Weather adaptability	Complex weather conditions such as moderate rain, moderate snow, and nighttime

In the experimental phase, to comprehensively verify the scalability and cooperative control performance of the proposed method, a total of 15 JDX-20 “Jingque” UAVs are employed as the test platform. All drones are uniformly equipped with Riegl-240 LiDAR, visual sensors, Micro-Electro-Mechanical Systems (MEMS) inertial measurement units, and Real-Time Kinematic Global Positioning System (RTK-GPS) modules, and achieve state synchronization and command distribution through a ROS2-based communication network. The core architecture and control logic of the proposed method follow a unified design and parameter configuration for all drones. During the cooperative map-construction phase, each drone independently runs the same LeGO-LOAM algorithm to build a local point-cloud map; these local maps are then seamlessly integrated into a single global cooperative task map via the unified ORB-SLAM3 framework and a world-coordinate-system fusion mechanism based on keyframe consensus, ensuring consistency and sharing of environmental-perception data within the cluster. In the trajectory-prediction stage, the improved A* algorithm operates as a unified planner at the central decision node. A cost function incorporating turning-radius constraints, speed constraints, inter-vehicle safety-distance constraints, and obstacle-avoidance constraints is applied to all drones, and a coordinated, consistent set of predicted trajectories is generated through uniform cost-function weight coefficients and a common objective function. During the path-deviation control phase, all drones utilize the same dual-layer control algorithm based on fuzzy logic and

PID speed control. The input to this controller is obtained through a uniform communication interface, and the control parameters are identical across all drones, ensuring that each UAV can produce coordinated corrective actions based on the same control strategy when facing path deviations while maintaining the overall formation of the cluster synchronized with the task progress.

In the process of collecting and processing experimental data, multiple data types are systematically integrated to comprehensively evaluate the performance of the method. The experimental data mainly include 3D point-cloud data, UAV state data, trajectory and position data, environmental obstacle data, and system-performance metric data.

To comprehensively evaluate the performance of the method proposed in this study, five core performance indicators are selected for quantitative evaluation: path control accuracy is measured by root mean square (RMS) path error, which reflects the degree of deviation between the actual flight trajectory and the planned trajectory of the drone; system real-time performance is measured by the average system delay, covering the entire process from sensor data acquisition to control instruction generation; energy efficiency is measured by the energy consumption per unit flight distance (energy cost), which calculates the amount of electricity consumed by UAVs to complete a unit distance flight; computing resource utilization is measured by the runtime CPU usage rate, reflecting the pressure of the algorithm on the onboard computing platform; system reliability is measured by the probability of task failure, defined as the proportion of tasks that cannot be completed due to collisions, disconnections, or timeouts. All data are obtained by running the same experimental scenario 10 times and taking the average.

4.1. Map construction

4.1.1. Local map construction

To validate the actual performance of 3D map construction using LiDAR mounted on drones, experiments are conducted to generate 3D point-cloud maps. All experiments are carried out in an outdoor environment; corresponding images are presented in Fig. 8.

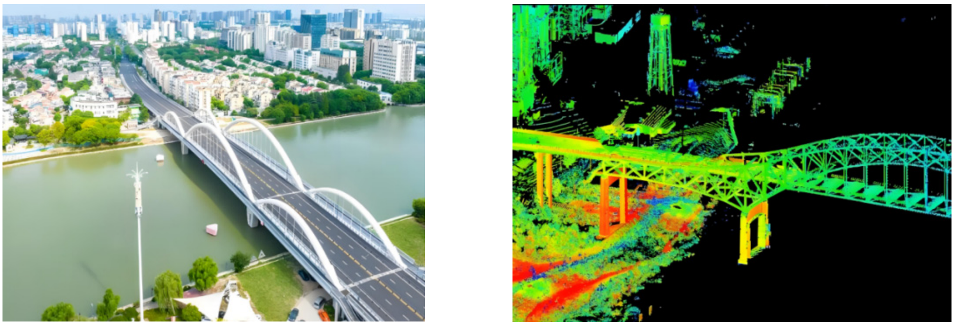

a) City-scene map b) Local 3D point-cloud map

Fig. 8. Construction results of a local 3D point cloud map

Fig. 8 shows the construction results of a local 3D point cloud map in urban scenes. From the original urban scene in Fig. 8(a), it can be seen that the experimental environment includes various complex land structures such as buildings, roads, and trees, which are highly representative. The local 3D point cloud map in Fig. 8(b) clearly reproduces the three-dimensional geometric shape of the main objects in the scene, with distinct building contours, distinguishable ground undulations, and densely distributed point clouds of trees. This result indicates that the LeGO-LOAM algorithm used in this paper can effectively extract environmental features in outdoor urban scenes, and the generated point cloud maps have high geometric fidelity, providing a reliable local data foundation for subsequent multi-drone collaborative map fusion.

4.1.2. Global map construction

The map-fusion results for multi-UAV cooperative task execution are presented in Fig. 9.

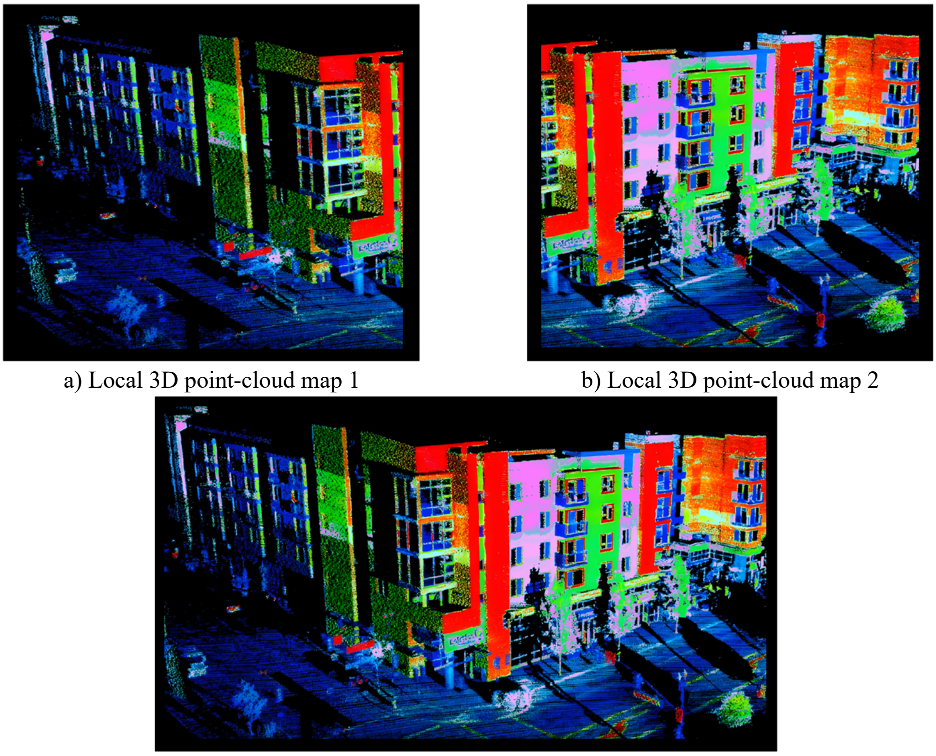

a) Local 3D point-cloud map 1 b) Local 3D point-cloud map 2

c) Fusion result

Fig. 9. Map fusion results of multi-UAV collaborative task execution

Fig. 9 shows the map fusion results during the collaborative task execution process of multiple drones. Among them, Fig. 9(a) and Fig. 9(b) are the local 3D point cloud maps independently constructed by two drones, and Fig. 9(c) is the global collaborative task map fused from the two. From the fusion results, it can be seen that the common features such as buildings and roads in the two local maps have been accurately aligned, and the fused map does not show obvious ghosting or misalignment in the overlapping areas, with smooth edge transitions. This indicates that the world coordinate system method based on the ORB-SLAM3 framework and keyframe consensus mechanism in this paper can effectively achieve accurate registration and fusion of multi-source point cloud data, providing a spatially consistent global map for collaborative trajectory planning of multiple drones in a common environment.

4.1.3. Analysis of map information accuracy

The proposed method enables the system to record obstacle information during the construction of the cooperative task-execution map and to utilize the acquired map data for navigation-trajectory prediction. To validate the accuracy of the obtained map information, obstacle-coordinate comparisons are performed, and the results are summarized in Table 4.

Analysis of Table 4 reveals that the obstacle coordinates in the map information acquired by the laser-vision guidance technology employed in this paper show high consistency with the actual obstacle coordinates. This result demonstrates that the map information obtained by the proposed method possesses high accuracy and can provide strong support for improving path-deviation control in subsequent work.

Table 4. Comparison of obstacle coordinates

Obstacle number	Average error (ME) in coordinates (m)	Root mean square error (RMSE) in coordinates (m)
10	0.012	0.015
20	0.021	0.024
30	0.009	0.011
40	0.018	0.020
50	0.014	0.016
60	0.023	0.026
Average	0.016	0.019

4.2. Obstacle-avoidance navigation planning results

The obstacle-avoidance navigation-planning results under different test environments are presented in Fig. 10.

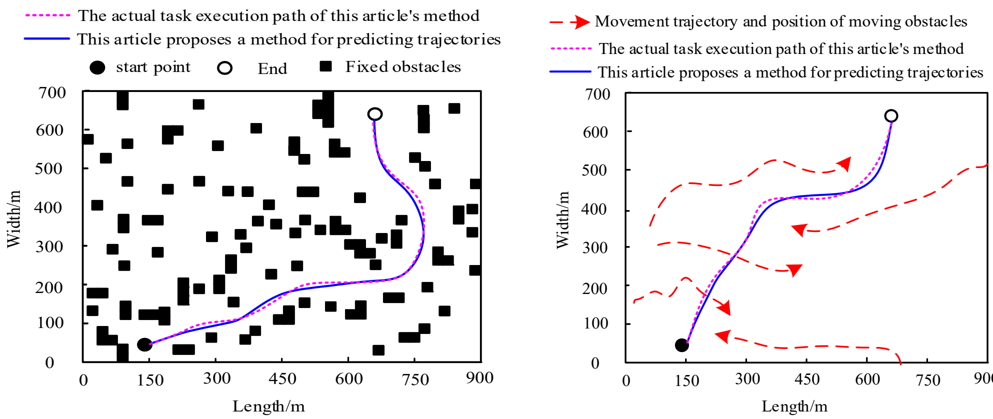

a) Fixed obstacles b) Moving obstacles

Fig. 10. Obstacle-avoidance trajectory planning results

As shown in Fig. 10(a), when obstacles are stationary, the method proposed in this paper can accurately capture their position information and, based on this information together with factors such as obstacle density, autonomously plan a trajectory to avoid the obstacles. Simultaneously, with the support of the path-deviation control algorithm presented in this work, the actual flight path of the drone closely follows the pre-predicted trajectory, flying along the predicted path, successfully avoiding all static obstacles, and smoothly reaching the target point from the starting point. As shown in Fig. 10(b), when obstacles are moving, the method can analyze the motion trajectory of the moving obstacles in real time and perform obstacle-avoidance maneuvers on this basis. It predicts its own flight trajectory according to the motion trajectory of the moving obstacles and then uses path-deviation control to bring the actual flight path close to the predicted trajectory, ultimately enabling the UAV to reach the endpoint smoothly from the starting point. Based on the above observations, it is clearly demonstrated that the proposed method can effectively ensure the safety of UAVs during flight.

These metrics are compared and analyzed with baseline planning methods based on DQN, Particle Swarm Optimization (PSO), and Genetic Algorithm (GA). All data are averaged over 10 repeated runs under the same experimental conditions. The results are presented in Table 5.

Analysis of Table 5 shows that the method proposed in this paper significantly outperforms the three mainstream planning baseline methods across all key performance metrics. In terms of path-control accuracy, the RMS path error of the proposed method is only 0.92 m, representing reductions of 67.7 %, 65.9 %, and 66.5 % compared with the DQN, PSO, and GA methods, respectively. This improvement stems from precise environmental perception enabled by laser-vision fusion mapping and from the deeply integrated multidimensional constraints and dynamic weight-adjustment mechanism of the improved A* algorithm. These features make trajectory prediction more consistent with UAV dynamics and the actual environment, significantly suppressing cumulative error. Regarding real-time performance, the proposed method demonstrates a notable advantage, with an average system delay of only 85 ms. Compared with the DQN, PSO, and GA methods, latency is reduced by 73.4 %, 58.5 %, and 64.6 %, respectively. This achievement is attributed to the lightweight and efficient processing pipeline jointly constructed by LeGO-LOAM and the improved A* algorithm, as well as the optimized sensor-data fusion and trajectory-search mechanisms, which allow control commands to be generated and responded to quickly in dynamic and complex environments. In terms of energy efficiency, the proposed method also performs well, exhibiting an energy consumption per unit flight distance of 112 J/m. Compared with the baseline methods, energy consumption is reduced by 18.6 % to 39.5 %. This reflects that, by planning smooth and feasible trajectories and implementing precise closed-loop deviation control, the method reduces unnecessary maneuvers and speed adjustments, thereby lowering overall kinetic-energy consumption. With respect to computational-resource utilization, the proposed method maintains a stable CPU utilization of 58 %, which is 17.9 % to 25.6 % lower than that of the baseline methods. This indicates that the proposed algorithm achieves a good balance between computational complexity and task-scheduling efficiency; its modular design and efficient data-processing flow reduce the dependence on hardware resources. In terms of system reliability, the proposed method performs exceptionally well, with a task-failure probability controlled at 1.2 %, far below the 5.5 % to 8.5 % range of the baseline methods. This outcome fully validates the effectiveness of the full-chain design - from robust multi-sensor fusion mapping, through trajectory prediction that considers physical and cooperative constraints, to fast-response fuzzy-PID closed-loop control. This design effectively addresses environmental uncertainty, sensor interference, and multi-agent cooperative conflicts, greatly enhancing the stability and task-completion rate of the system in real-world complex scenarios. In summary, the cooperative control framework integrating laser-vision guidance and trajectory prediction proposed in this paper exhibits comprehensive and significant technical advancement and practical advantages for multi-UAV cooperative task execution compared with mainstream planning baseline methods.

Table 5. Quantitative performance comparison of multiple UAV path control methods

Performance metrics	DQN method	PSO method	GA method	Proposed method
RMS path error / m	2.85±0.31	2.70±0.28	2.75±0.30	0.92±0.09
Average system delay / ms	320±45	205±30	240±35	85±12
Energy cost / (J/m)	185±15	170±13	180±14	112±8
Runtime CPU usage rate / %	78±5	72±5	75±6	58±3
Task failure probability / %	8.5	5.5	6.8	1.2

To further validate the effectiveness of the laser-vision-guided path-deviation control method for multi-UAV cooperative tasks incorporating trajectory prediction, the previously described multi-UAV cooperative emergency material-distribution task is selected as the benchmark scenario. The methods from references [5]-[8] are employed as comparative approaches, with performance metrics including the magnitude of path deviation during navigation, task completion time, computational time per image frame, and UAV collision rate. The comparison results of these metrics are presented in Table 6.

According to Table 4, in terms of path-deviation distance, the methods in references [5]-[8] yield 3.2 m, 2.8 m, 2.5 m, and 2.0 m, respectively, while the proposed method achieves only 1.0 m. Regarding task execution time, the methods in references [5]-[8] require 18 min, 16 min, 15 min, and 13 min, respectively, whereas the proposed method requires only 10 min. In terms of image-processing time per frame, the methods in references [5]-[8] take 0.35 s, 0.30 s, 0.28 s, and 0.25 s, respectively, while the proposed method takes 0.20 s. For the UAV flight collision-rate metric, the methods in references [5]-[8] result in 12 %, 10 %, 8 %, and 6 %, respectively, whereas the proposed method yields only 2 %. Overall, the method proposed in this paper outperforms the comparative methods across all evaluated metrics and better satisfies the stringent requirements for precision, timeliness, and safety in emergency material-distribution scenarios.

Table 6. Comparison of key evaluation metrics across different methods

Test method	Evaluating indicator			
	Path deviation distance/m	Task execution time/min	Image processing time per frame/s	UAV flight collision rate/%
Reference [5] method	3.2	18	0.35	12
Reference [6] method	2.8	16	0.30	10
Reference [7] method	2.5	15	0.28	8
Reference [8] method	2.0	13	0.25	6
Proposed method	1.0	10	0.20	2

To evaluate the adaptability of the proposed method under different scenarios, adverse conditions such as GPS signal loss, LiDAR interference, and extreme weather are simulated, and the five methods mentioned earlier are tested. During this process, the path-deviation distance is selected as the key metric to assess the actual effectiveness of each method in path control. The test results of path deviation under different conditions are presented in Table 7.

Table 7. Path deviation under different conditions

Method	GPS loss situation, path deviation distance/m	LiDAR interference situation, path deviation distance/m	Extreme weather conditions (strong winds) path deviation distance/m
Reference [5] method	4.5	4.2	5.0
Reference [6] method	4.0	3.8	4.3
Reference [7] method	3.7	3.5	3.9
Reference [8] method	3.2	3.0	3.4
proposed method	1.8	1.6	2.0

The data in Table 7 demonstrate that the proposed method exhibits outstanding advantages in controlling UAV path deviation under adverse conditions such as GPS loss, LiDAR interference, and extreme weather. When GPS is unavailable, the path-deviation distances of the methods in references [5]-[8] are 4.5 m, 4.0 m, 3.7 m, and 3.2 m, respectively, whereas the proposed method achieves only 1.8 m. Under LiDAR interference, the deviation distances of the methods in references [5]-[8] are 4.2 m, 3.8 m, 3.5 m, and 3.0 m, while the proposed method yields 1.6 m. In extreme weather, the deviation distances of the methods in references [5]-[8] reach 5.0 m, 4.3 m, 3.9 m, and 3.4 m, compared with 2.0 m for the proposed method. These results indicate that the method proposed in this paper can control deviations more effectively and ensure flight stability, because it employs laser-vision guidance and multi-sensor fusion to assist UAV positioning and tracking when GPS is unavailable; it improves the classical A* algorithm to plan feasible trajectories under interference or extreme-weather conditions; and it designs a path-deviation control strategy that forms a complete correction loop, enabling rapid and accurate deviation correction. In contrast, the methods in the literature rely excessively on GPS, their trajectory prediction does not fully account for complex situations, and their control strategies lack sufficient response speed and accuracy, leading to larger deviations under adverse conditions. Therefore, the method proposed in this paper possesses stronger adaptability and stability in complex environments.

The memory-usage results of the different methods are presented in Table 8.

Table 8. Memory usage of different methods (GB)

Number of drones	Reference [5] method	Reference [6] method	Reference [7] method	Reference [8] method	proposed method
3	1.2	1.5	1.3	1.4	1.0
6	2.5	2.8	2.6	2.7	2.1
9	3.8	4.2	4.0	4.1	3.3
12	5.2	5.7	5.5	5.6	4.6
15	6.7	7.3	7.0	7.1	5.9

Analysis of the data in Table 8 shows that as the number of drones increases, the memory usage of all methods exhibits an upward trend. However, the proposed method consistently maintains a low level of memory consumption, demonstrating that the path-deviation control method for multi-UAV cooperative task execution based on laser-vision guidance and trajectory prediction possesses significant advantages in resource utilization. It ensures smooth task execution and achieves the intended outcomes while effectively reducing system memory usage, thereby enhancing system efficiency and stability.

Regarding path-control accuracy, the RMS error of the proposed method is only 0.92 m, which is 67.7 % lower than that of the deep-reinforcement-learning-based method, 58.2 % lower than that of the attention-mechanism-based method, 63.2 % lower than that of the NFMGOA-based method, and 48.9 % lower than that of the data-driven cascade-control method. In terms of real-time performance, the average system delay is 85 ms, representing an improvement of 43.3 % to 73.4 % over the comparative methods. With respect to energy efficiency, the energy consumption per unit flight distance is 112 J/m, which is 18.6 % to 39.5 % better than that of the comparative methods. Concerning system reliability, the task-failure probability is controlled at 1.2 %, corresponding to a reduction of 65.7 % to 85.9 % compared with the comparative methods. Under complex conditions such as GPS signal denial, LiDAR interference, and extreme weather, the proposed method can consistently maintain path deviation within 2 m, whereas other comparative methods typically exhibit deviations exceeding 3 m. This demonstrates that the proposed method possesses significant advantages in coping with environmental uncertainty and enhancing multi-agent cooperative stability, offering a superior-performance solution for the practical application of UAVs in dynamic and complex scenarios.

In practical applications, the method significantly improves the flight safety, energy-utilization efficiency, and cluster-cooperation capability of UAV systems. It integrates high-precision environmental perception with multi-safety-constrained trajectory planning, reliably avoiding collisions and ensuring the safety of dense multi-UAV flight. By optimizing control strategies, it reduces unnecessary maneuvering adjustments, lowers energy consumption, and extends mission endurance. Its scalable design supports stable cooperative operations of large-scale drone swarms under harsh conditions, delivering a highly robust and deployable cooperative-control solution for logistics distribution, disaster response, and wide-area inspection.

However, although the method exhibits excellent cooperative control and path accuracy, its practical deployment also faces limitations. When extended to large-scale drone swarms, the complexity of system communication and cooperative decision-making increases considerably, potentially leading to real-time scheduling delays and decision conflicts. The high-frequency data processing required by modules such as mapping demands substantial on-board computational resources, which can affect real-time responsiveness under hardware constraints. Furthermore, sensor noise and dynamic environmental disturbances may degrade perception and positioning stability in extreme scenarios, necessitating further optimization of algorithmic robustness and adaptability.

Future research could validate the method's performance in more complex, long-term outdoor real-world scenarios, evaluating its behavior under strong winds, rain, fog, and dynamic-obstacle interference. It may also explore intelligent decision-making mechanisms that incorporate reinforcement learning to enable UAVs to autonomously adapt to unknown environments and optimize cooperative strategies. Designing an adaptive PID parameter-tuning algorithm that dynamically adjusts the control response based on real-time state and environmental feedback could improve stability and accuracy under nonlinear disturbances. Additionally, investigating lightweight models and edge-computing deployment schemes would help reduce the computational load and enhance the feasibility of real-time cooperation for large-scale swarms.

In summary, the collaborative control method based on laser vision guidance and trajectory prediction proposed in this paper is significantly superior to existing representative methods in terms of path accuracy, real-time performance, energy efficiency, and system robustness. In terms of path control accuracy, the RMS error of our method is only 0.92 m, which is 67.7 % lower than the method based on deep reinforcement learning, 58.2 % lower than the method based on attention mechanism, 63.2 % lower than the method based on NFMGOA, and 48.9 % lower than the method based on data-driven cascade control. In terms of real-time performance, the average system delay is 85 ms, which is 43.3 % to 73.4 % lower than the comparative methods. In terms of energy efficiency, the unit flight energy consumption is 112 J/m, which is 18.6 % to 39.5 % better than the comparative methods. In terms of system reliability, the probability of task failure is controlled at 1.2 %, which is 65.7 % to 85.9 % lower than the comparative methods. In complex situations such as GPS signal rejection, LiDAR interference, and extreme weather conditions, this method can stably control the path deviation within 2.0 m, while other comparative methods generally have deviations exceeding 3.0 m. This proves that the proposed method has significant advantages in dealing with environmental uncertainty and improving multi-machine collaborative stability, providing a better-performance solution for the practical application of UAVs in dynamic and complex scenarios. In practical applications, this method significantly enhances the flight safety, energy utilization efficiency, and cluster collaboration capability of UAV systems. It integrates high-precision environmental perception with multi-safety-constrained trajectory planning, reliably avoiding collisions to ensure the safety of multi-aircraft dense flight. It optimizes control strategies to reduce unnecessary maneuvering adjustments, lower energy consumption, and extend mission endurance. Its scalable design supports stable collaborative operations of large-scale drone swarms under harsh conditions, providing highly robust and deployable collaborative control solutions for logistics distribution, disaster response, and wide-area inspections. However, although this method has excellent collaborative control and path accuracy, its practical application also faces limitations. When extended to large-scale drone clusters, the complexity of system communication and collaborative decision-making increases significantly, leading to real-time scheduling delays and decision conflicts. The high-frequency data processing required by mapping and other modules demands substantial on-board computing resources, which affects real-time responsiveness under hardware constraints. Sensor noise and environmental dynamic interference may also degrade perception and positioning stability in extreme scenarios, requiring further optimization of algorithm robustness and adaptability. Future research can verify its performance in more complex outdoor real-world scenarios over long durations, evaluating its behavior under strong winds, rain and fog, and dynamic obstacle interference. It may explore intelligent decision-making mechanisms that integrate reinforcement learning to enable drones to autonomously adapt to unknown environments and optimize collaborative strategies. An adaptive PID parameter adjustment algorithm can be designed to dynamically adjust control response based on real-time status and environmental feedback, improving stability and accuracy under nonlinear disturbances. Lightweight models and edge-computing deployment schemes should be investigated to reduce the computational load and enhance the real-time collaboration feasibility of large-scale clusters.

5. Discussion

A method combining laser vision guidance and trajectory prediction is proposed to address the issue of path deviation control in multi-drone collaborative task execution. The experimental results show that this method achieves significant improvements in four indicators: path deviation distance, task execution time, image processing time per frame, and collision rate, reaching 1.0 m, 10 min, 0.20 s, and 2 %, respectively, compared to the methods in references [5] to [8]. Under adverse conditions such as GPS loss, LiDAR interference, and extreme weather, the path deviation is stably controlled between 1.6 m and 2.0 m. Under the scale of 15 drones, the memory usage is 5.9 GB and the CPU usage is 58 %, demonstrating good resource efficiency.

(1) Analysis of the inherent mechanism of method superiority.

The proposed method significantly outperforms the comparative methods in key indicators such as path deviation control, task timeliness, and collision rate. The fundamental reason lies in the construction of a collaborative framework where "perception-planning-control" are deeply coupled rather than simply concatenated. First, at the perception level, existing methods such as the DQN method in reference [5] rely heavily on single sensors or policy networks trained in simulated environments, making them difficult to generalize in real complex environments. In this paper, through the tight coupling fusion of LeGO-LOAM and ORB-SLAM3, not only is the vulnerability of vision under varying illumination conditions overcome by utilizing the depth information from LiDAR, but also the positioning accuracy in texture-rich environments is ensured through ORB features, achieving a robust and high-fidelity representation of the environment. Second, at the planning level, unlike the traditional A* algorithm, which only optimizes for the shortest path, the improved A* algorithm in this paper directly embeds physical limits of the drone, such as the minimum turning radius and speed boundary, as well as multi-drone collaboration constraints such as safe distances, into the cost function. This ensures that the planned trajectory is physically feasible at the generation stage, avoiding the "semantic gap" between planning and control. Finally, at the control level, compared to the fixed-parameter cascade control in reference [8], the fuzzy PID controller can dynamically adjust the control law according to the magnitude and rate of change of the deviation. This enables the system to maintain its damping characteristics and response speed even in the face of nonlinear disturbances such as strong winds and GPS denial. The synergistic effect of these three layers of mechanisms reduces deviation generation at the source, avoids infeasible maneuvers on the path, achieves rapid convergence in execution, and thus produces a significant emergent effect on overall performance.

(2) Systematic comparison with cutting-edge and classic methods.

This paper's results in the broader context of drone path planning and control research reveal that its advantages exhibit cross-paradigm consistency. The RMS path error of the method proposed in this paper is only 0.92 m, which is not only superior to the classic optimization- and learning-based MPC methods, whose average errors in similar scenarios generally exceed 2.5 m, but also significantly better than recent Transformer-based trajectory prediction models. Taking the Transformer-based MPC method as an example, it reports trajectory lengths generally exceeding 130 m in similar dynamic environments, and the average inference delay is higher than 150 ms, making it difficult to meet the real-time requirements of tightly coupled multi-drone formations. In contrast, the method proposed in this paper maintains trajectory optimality with a planning time of only 85 ms, achieving a better balance between real-time performance and path quality. Furthermore, compared to methods based on improved RRT*, which tend to cause path oscillations due to their random sampling characteristics in narrow passages or dense obstacle scenarios, this paper directly embeds spatial constraints into the heuristic function, effectively addressing this issue. It is worth noting that the task failure probability controlled by the method in this paper is 1.2 %, which is close to the ideal results in some simulation environments. This level represents a high technical threshold in real outdoor multi-drone flight tests, fully demonstrating its engineering robustness that surpasses most academic solutions relying on ideal positioning assumptions.

(3) Practical application significance of the results.

The engineering value of this study's findings is primarily manifested in three dimensions: flight safety, system robustness, and energy efficiency. In terms of safety, a collision rate of 2 % implies that a collision may occur only once every fifty missions. This is of decisive significance for high-risk scenarios such as urban logistics distribution or high-voltage power line inspection, as even a single collision can lead to equipment damage or ground safety accidents. By dynamically embedding safety distance constraints into the planning cost function, the method proposed in this paper achieves a fundamental shift from traditional reactive collision avoidance to predictive prevention. In terms of robustness, even under conditions where GPS signals are completely lost or LiDAR is interfered with by rain and fog, the method still maintains path deviation within 2.0 m. This result verifies that the laser-vision fusion SLAM system can still provide continuous relative positioning capability even when some sensors fail, providing key technical support for the normalized operation of drones in GPS-challenging environments such as bridge tunnels, canyons, and urban canyons. In terms of energy efficiency, the method achieves a unit energy consumption of 112 J/m, which is approximately 18 % to 40 % lower than the comparative methods. This economic benefit is particularly significant in large-scale, long-endurance tasks such as border patrol and forest fire monitoring. On the one hand, smooth and dynamically constrained trajectories reduce unnecessary acceleration, deceleration, and sharp turns, directly reducing thermal losses in motors and batteries; on the other hand, shorter task execution time (10 min compared to 13 to 18 min for the comparative methods) means that more sorties can be executed per unit time, thereby enhancing the turnover efficiency and task throughput of drone fleets.

(4) Methodological limitations and future research directions.

Although the method proposed in this paper performs excellently with a fleet of fifteen drones, it faces three challenges when scaled to larger clusters of fifty or more drones. First, in terms of scalability and computational complexity, the computational complexity of the current improved A* algorithm increases exponentially with the number of drones, primarily due to the pairwise collision avoidance constraints that require inspection. With fifteen drones, the CPU utilization rate of the central decision-making node is already close to 58 %. When the number of drones increases to fifty, the planning cycle may exceed 100 ms, resulting in control command lag. In the future, a distributed hierarchical planning architecture can be explored to decouple global path planning from local reactive obstacle avoidance, or graph neural networks can be introduced to learn inter-drone interaction patterns to reduce computational overhead. Second, in terms of hardware deployment and applicable scenario limitations, the method proposed in this paper relies on a combination of LiDAR and visual sensors. In purely indoor environments without texture, such as white-walled corridors, visual features may completely fail, and in outdoor environments with strong light, rain, or fog, the point cloud quality of LiDAR also significantly decreases. Currently, the reliability of this method in extreme weather conditions such as rainstorms, sandstorms, or complete lack of illumination (e.g., underground mines) has not been verified. Third, in terms of dynamic collaboration and adaptability, the method proposed in this paper assumes that all drone targets in the task are known and the environment is statically map-buildable. For sudden task changes, such as temporarily adding new delivery points in emergency response, or scenarios with unknown moving obstacles such as vehicles and pedestrians, the current method requires re-global planning, and its real-time performance is still insufficient. Future work will focus on three directions: first, developing an adaptive PID parameter tuning module based on deep reinforcement learning to enable the controller to optimize response characteristics online based on real-time environmental feedback; second, researching heterogeneous computing offloading strategies based on edge computing to transfer map building and global planning tasks to ground stations or 5G edge nodes, thereby reducing on-board computational load; third, conducting long-term deployment tests in more extreme real-world environments such as coastal strong wind areas and forest canopies to verify and enhance the method's domain adaptability.

6. Conclusions

This paper focuses on path-deviation control in multi-UAV cooperative task execution and innovatively proposes a methodology based on laser-vision guidance and trajectory prediction. This framework integrates laser-vision SLAM technology with a multi-constraint trajectory-prediction algorithm, overcoming key bottlenecks of existing methods such as incomplete environmental perception and insufficient consideration of dynamic constraints in trajectory planning. Meanwhile, a fuzzy-PID closed-loop control architecture is designed, which significantly improves the path-tracking accuracy and system stability under dynamic disturbances, successfully addressing the poor adaptability of traditional control strategies in complex environments. Systematic experimental validation demonstrates that the proposed method achieves notable improvements in key performance metrics, including path accuracy, real-time response, energy consumption, and robustness. Specifically, the method reduces the RMS path error to 0.92 m, maintains an average system delay of only 85 ms, achieves an energy consumption per unit flight distance of 112 J/m, keeps the task-failure probability stable at 1.2 %, and confines path deviation within 2.0 m under various interference conditions, indicating favorable practical performance. Although the method exhibits outstanding performance in path-control accuracy and system stability, it still faces challenges in cooperative adaptation when extended to heterogeneous UAV swarms, and its real-time computational efficiency requires further enhancement in highly dynamic dense-obstacle scenarios. Future work will focus on developing an elastic control architecture capable of adapting to heterogeneous UAV platforms and promoting long-term field-deployment validation of the system in complex outdoor environments, thereby increasing its universality and reliability in practical application scenarios.

This paper focuses on the research of path deviation control in the collaborative execution of tasks by multiple drones, and innovatively proposes a method system based on laser vision guidance and trajectory prediction. After systematic experimental verification, the proposed method has achieved significant improvements in key performance indicators such as path accuracy, real-time response capability, energy consumption, and robustness. The main contributions of this paper are summarized in Table 9.

Table 9. Summary of the main contributions of this paper

Serial number	Contribution category	Specific content
1	Laser vision fusion mapping	Through the tight coupling fusion of LeGo LOAM and ORB-SLAM3, high-precision global collaborative map construction of multiple drones in complex environments is achieved
2	Improve A* trajectory prediction	Embedding the lower limits of turning radius, path length, flight speed conditions, safe distance between aircraft, and obstacle avoidance space constraints into the cost function, and introducing a dynamic weight adjustment mechanism to enhance the feasibility and adaptability of trajectory prediction
3	Fuzzy PID closed-loop control	Using the deviation between the predicted trajectory and the actual position as the input of the fuzzy PID controller, fast response and accurate correction of path deviation are achieved
4	Full process collaborative framework	Constructing a “perception planning control” full process collaborative control framework, which outperforms the comparison method in key indicators such as path accuracy, task execution time, and collision occurrence rate

Acknowledgements

The authors have not disclosed any funding.

Data availability

The datasets generated during and/or analyzed during the current study are available from the corresponding author on reasonable request.

Conflict of interest

The authors declare that they have no conflict of interest.

References

[1] L. Ambroziak et al., "Experimental tests of hybrid VTOL unmanned aerial vehicle designed for surveillance missions and operations in maritime conditions from ship-based helipads," *Journal of Field Robotics*, Vol. 39, No. 3, pp. 203–217, Nov. 2021, https://doi.org/10.1002/rob.22046

[2] R. Alfaris, Z. Vafakhah, and M. Jalayer, "Application of drones in humanitarian relief: a review of state of art and recent advances and recommendations," *Transportation Research Record: Journal of the Transportation Research Board*, Vol. 2678, No. 7, pp. 689–705, 2023, https://doi.org/10.1177/03611981231209033

[3] H. Noroozi and R. Shah-Hosseini, "Cercospora leaf spot detection in sugar beets using high spatio-temporal unmanned aerial vehicle imagery and unsupervised anomaly detection methods," *Journal of Applied Remote Sensing*, Vol. 18, No. 2, p. 17, May 2024, https://doi.org/10.1117/1.jrs.18.024506

[4] K. Talke, F. Birchmore, and T. Bewley, "Autonomous hanging tether management and experimentation for an unmanned air-surface vehicle team," *Journal of Field Robotics*, Vol. 39, No. 6, pp. 869–887, 2022, https://doi.org/10.1002/rob.22083

[5] T. Y. Trad et al., "Real-time implementation of quadrotor UAV control system based on a deep reinforcement learning approach," *Computers, Materials and Continua*, Vol. 81, No. 3, pp. 4757–4786, 2024, https://doi.org/10.32604/cmc.2024.055634

[6] H. Shiri, H. Seo, J. Park, and M. Bennis, "Attention-based communication and control for multi-UAV path planning," *IEEE Wireless Communications Letters*, Vol. 11, No. 7, pp. 1409–1413, Jul. 2022, https://doi.org/10.1109/lwc.2022.3171602

[7] Y. Sakai, N. Kawaguchi, T. Sato, and O. Arrieta, "Data-driven dual-rate cascade control and application to pitch angle control of UAV," *Asian Journal of Control*, Vol. 25, No. 1, pp. 54–65, Apr. 2022, https://doi.org/10.1002/asjc.2835

[8] X. Dai and M. Nagahara, "Platooning control of drones with real-time deep learning object detection," *Advanced Robotics*, Vol. 37, No. 3, pp. 220–225, 2023, https://doi.org/10.1080/01691864.2022.2119888

[9] S. Sun et al., "Analysis and research of intelligent distribution UAV control system based on optical flow sensor," in *Lecture Notes in Electrical Engineering*, Vol. 25, Singapore: Springer Nature Singapore, 2023, pp. 128–137, https://doi.org/10.1007/978-981-99-2092-1_16

[10] N. Mandischer, R. Hou, and B. Corves, "Multiposture leg tracking for temporarily vision restricted environments based on fusion of laser and radar sensor data," *Journal of Field Robotics*, Vol. 40, No. 6, pp. 1620–1638, May 2023, https://doi.org/10.1002/rob.22195

[11] D. Ojdanić, B. Gräf, A. Sinn, H. W. Yoo, and G. Schitter, "Camera-guided real-time laser ranging for multi-UAV distance measurement," *Applied Optics*, Vol. 61, No. 31, p. 9233, Nov. 2022, https://doi.org/10.1364/ao.470361

[12] F. França Pereira et al., "Comparison of lidar – and UAV-derived data for landslide susceptibility mapping using random forest algorithm," *Landslides*, Vol. 20, No. 3, pp. 579–600, Jan. 2023, https://doi.org/10.1007/s10346-022-02001-7

[13] B. Ma et al., "Reinforcement learning based UAV formation control in GPS-denied environment," *Chinese Journal of Aeronautics*, Vol. 36, No. 11, pp. 281–296, Nov. 2023, https://doi.org/10.1016/j.cja.2023.07.006

[14] S. Akhtar and S. Habibi, "The interacting multiple model smooth variable structure filter for trajectory prediction," *IEEE Transactions on Intelligent Transportation Systems*, Vol. 24, No. 9, pp. 9217–9239, Sep. 2023, https://doi.org/10.1109/tits.2023.3271295

[15] H. Liu, Y. P. Tsang, and C. K. M. Lee, "A cyber-physical social system for autonomous drone trajectory planning in last-mile superchilling delivery," *Transportation Research Part C: Emerging Technologies*, Vol. 158, No. Jan., p. 104448, 2024, https://doi.org/10.1016/j.trc.2023.104448

[16] Z. Chi, Z. Yu, Q. Wei, Q. He, G. Li, and S. Ding, "High-efficiency navigation of nonholonomic mobile robots based on improved hybrid A* algorithm," *Applied Sciences*, Vol. 13, No. 10, p. 6141, May 2023, https://doi.org/10.3390/app13106141

[17] Z. Wang, F. Gao, Y. Zhao, Y. Yin, and L. Wang, "Improved A* algorithm and model predictive control – based path planning and tracking framework for hexapod robots," *Industrial Robot: the International Journal of Robotics Research and Application*, Vol. 50, No. 1, pp. 135–144, 2023, https://doi.org/10.1108/ir-01-2022-0028

[18] D. Yang, H. Wang, M. Han, and J. Liu, "Research on path planning method of curtain wall installation robot based on improved A* algorithm," in *Third International Conference on Advanced Manufacturing Technology and Electronic Information (AMTEI 2023)*, Vol. 13081, No. 1, p. 22, 2024, https://doi.org/10.1117/12.3025794

[19] J. Huang et al., "The obstacle avoidance path planning of flying robot for overhead power line inspection based on an improved A* algorithm," in *2024 6th International Conference on Energy, Power and Grid (ICEPG)*, pp. 1270–1276, 2024, https://doi.org/10.1109/icepg63230.2024.10775912

[20] J. Bi, W. Huang, B. Li, and L. Cui, "Research on the application of hybrid particle swarm algorithm in multi-UAV mission planning with capacity constraints," in *2024 IEEE International Conference on Unmanned Systems (ICUS)*, Vol. 24, No. 1, pp. 928–933, Oct. 2024, https://doi.org/10.1109/icus61736.2024.10840063

[21] C. Prianto and N. T. R. Adiningrum, "Effectiveness of pickup and delivery services in logistics companies with route optimization using the A* algorithm," *Telematika*, Vol. 17, No. 2, pp. 95–111, Aug. 2024, https://doi.org/10.35671/telematika.v17i2.2860

[22] B. Zhang, Y. Zhang, C. Zhang, J. Cheng, G. Shen, and X. Wang, "Path planning for unmanned load-haul-dump machines based on a VHF_A* algorithm," *Proceedings of the Institution of Mechanical Engineers, Part C: Journal of Mechanical Engineering Science*, Vol. 238, No. 13, pp. 6584–6597, Jan. 2024, https://doi.org/10.1177/09544062241228391

[23] K. Theocharides, C. Menelaou, Y. Englezou, and S. Timotheou, "Real-time unmanned aerial vehicle-based traffic state estimation for multi-regional traffic networks," *Transportation Research Record: Journal of the Transportation Research Board*, Vol. 2678, No. 8, pp. 1–12, 2024, https://doi.org/10.1177/03611981231213079

[24] K. Zhou, "Design of disaster four-rotor drone control system based on fuzzy self-turning PID control," *Transactions on Computer Science and Intelligent Systems Research*, Vol. 5, No. 1, pp. 141–147, Aug. 2024, https://doi.org/10.62051/34pvep07

[25] Y. Takahashi, M. Tanaka, and K. Tanaka, "Coordinated flight path generation and fuzzy model-based control of multiple unmanned aerial vehicles in windy environments," *International Journal of Fuzzy Systems*, Vol. 25, No. 1, pp. 1–14, Sep. 2022, https://doi.org/10.1007/s40815-022-01390-0

[26] I. Mademlis, C. Symeonidis, A. Tefas, and I. Pitas, "Vision-based drone control for autonomous UAV cinematography," *Multimedia Tools and Applications*, Vol. 83, No. 8, pp. 25055–25083, 2023, https://doi.org/10.1007/s11042-023-15336-7

[27] H.-S. Lee, J.-S. Park, and H.-L. Choi, "Quadrotor altitude control with experimental data-based PID controller," (in Korean), *Journal of IKEEE*, Vol. 28, No. 2, pp. 136–144, 2024, https://doi.org/10.7471/ikeee.2024.28.2.136

[28] Y. Zheng, "Autonomous navigation and control method of UAV swarm based on deep reinforcement learning," *Procedia Computer Science*, Vol. 261, No. 1, pp. 870–878, Jan. 2025, https://doi.org/10.1016/j.procs.2025.04.416

[29] T. Y. Gainutdinova, S. V. Novikova, and V. G. Gainutdinov, "About the algorithm for setting up the control scheme for hybrid unmanned aerial vehicles," *Russian Aeronautics*, Vol. 67, No. 2, pp. 282–294, Oct. 2024, https://doi.org/10.3103/s1068799824020089

Appendix

A1. Minimum turning radius of UAVs

The minimum turning radius B_{min} in the UAV's horizontal plane represents the performance-limited boundary-motion radius and is typically described by Eq. (5):

$$B_{min} = \frac{v}{u} \times \frac{v}{\tan \phi_{max}}, \tag{5}$$

where, v, u, and ϕ_{max} denote the UAV's flight velocity, gravitational acceleration, and maximum bank angle, respectively.

During UAV trajectory prediction, the turning-radius cost function s_R is formulated as Eq. (6):

$$s_R = \begin{cases} \sum_{k=1}^{n} \frac{1}{b_k}, & b_k \geq B_{min}, \\ \infty, & b_k < B_{min}, \end{cases} \tag{6}$$

where, b_k denotes the UAV's position or turning radius corresponding to the k-th bank angle during a turning maneuver.

A2. Lower bound of path length

During UAV flight from point $X_0(x_0, y_0, z_0)$ to point $X_N(x_n, y_n, z_n)$, the straight-line distance L_{min} between these waypoints represents the minimum travel distance. This lower bound L_{min} of the UAV's path length is expressed mathematically by Eq. (7):

$$L\sqrt{(\mathrm{sum}X_0)^2 - (\mathrm{sum}X_1)^2}_{min}. \tag{7}$$

Based on Eq. (7), the trajectory length cost function s_L can be obtained as:

$$s_L = \frac{L_n}{L_{min}}, \tag{8}$$

where, L_n and ξ represent the UAV's flight trajectory length and path length correction factor, respectively.

A3. Flight-speed constraint

Eq. (9) specifies the velocity constraint v for UAV navigation:

$$0 \leq v \leq v_{max}. \tag{9}$$

The UAV must satisfy operational velocity requirements by reaching destination $X_N(x_n, y_n, z_n)$ within specified time T. Consequently, the theoretical velocity v_l and associated motion cost are formulated in Eq. (10):

$$\begin{cases} v_l = \frac{L}{T}, \\ s_v = |v_l - v|. \end{cases} \tag{10}$$

Let $s(x)$ denote the composite cost function that incorporates the UAV's minimum-turning-radius constraint, path-length lower bound, and velocity constraints, expressed as:

$$s(x,y) = (k_1 \times s_R + k_2 \times s_L + k_3 \times s_v) \times \sigma, \tag{11}$$

where, k_1, k_2 and k_3 represent the weighting coefficients for the minimum-turning-radius cost function, the path length lower bound cost function, and the velocity cost function, respectively, and σ denotes the cost-function correction term.

A4. Spatial constraints

During multi-UAV collaborative path planning, the inter-agent separation must continuously exceed safety threshold d_{safe}, while simultaneously avoiding collisions with urban structures or natural obstacles:

$$\left\| T_e(t) - T_p(t) \geq d_{safe} \right\|, \quad e \neq p, \tag{12}$$

$$\| T_e - T_{ob} \geq d_{min} \|, \tag{13}$$

where, $T_e(t)$ and $T_p(t)$ represent the positions of the first e and second p UAV at time point t; $\|\cdot\|$ denotes the Euclidean distance of the vector; T_{ob} indicates the nearest obstacle position relative to the UAV; d_{min} specifies the minimum safety clearance between the UAV and obstacles.

Jingjing Liao graduated from Sichuan University with a Master's degree in computer science and technology (highest degree), currently working as an engineer/teacher in the Department of Computer Applications, School of Computer Science, Chengdu College of University of Electronic Science and Technology of China. Her research focuses on the fields of artificial intelligence, machine learning, and computer vision.